

Calibration of DEM parameters for coated sunflower seeds based on dynamic stacking angle

Changji Liu, Wuyun Zhao, Bin Feng, Linrong Shi*, Bugong Sun, Fei Dai, Hui Li

(College of Mechanical and Electrical Engineering, Gansu Agricultural University, Lanzhou 730070, China)

Abstract: To address the errors associated with the application of existing Discrete Element Method simulation parameters in roller-type precision seeders, this study focused on calibrating the key contact parameters of the ‘Xinhe No. 1’ coated confectionary sunflower seeds, so as to provide a reliable simulation foundation for the optimization of the seeders. Through dynamic stacking angle experiments and comparative trials involving confectionary sunflowers (including Xinhe No. 1) and oil sunflowers with significantly different physical properties, the optimal working conditions for the rotating drum were determined as a rotation speed of 10 r/min, 304 Stainless Steel as the inner wall material, and a filling ratio of 30%. The study also clarified the variation patterns of the dynamic stacking angle. Physical experiments were conducted to measure the static friction coefficients, restitution coefficients, and inter-seed restitution coefficients between Xinhe No. 1 seeds and three materials: 304 Stainless Steel, Q235 Steel, and ABS Plastic. The physical dynamic stacking angle was obtained via a rotating drum experiment. A single-factor experiment was used to determine the range of simulation parameters, and a second-order orthogonal experiment was conducted using Design-Expert software to optimize contact parameters with the physical dynamic stacking angle as the target. The parameters were subsequently validated using the Discrete Element Method (DEM) simulation software EDEM 2022.3, hereinafter abbreviated as EDEM simulations. Finally, rolling friction coefficients between seeds and Q235 Steel and ABS Plastic were obtained through both simulation and physical experiments using alternative contact materials. The results showed that the static friction coefficients between Xinhe No. 1 and 304 Stainless Steel, Q235 Steel, and ABS Plastic were 0.32, 0.36, and 0.25, respectively; the restitution coefficients were 0.42, 0.39, and 0.32; and the rolling friction coefficients were 0.012, 0.011, and 0.010. The measured values of the inter-seed static friction coefficient, restitution coefficient, and rolling friction coefficient were 0.31, 0.43, and 0.010, respectively. The relative error between simulated and physical stacking angles was <1.5%. Calibrated DEM parameters for Xinhe No. 1 coated sunflower seeds provide a theoretical basis for optimizing the design of sunflower precision seeders.

Keywords: sunflower seed, DEM, parameter calibration, dynamic stacking angle, hill-drop planter

DOI: [10.25165/j.ijabe.20261901.10103](https://doi.org/10.25165/j.ijabe.20261901.10103)

Citation: Liu C J, Zhao W Y, Feng B, Shi L R, Sun B G, Dai F, et al. Calibration of DEM parameters for coated sunflower seeds based on dynamic stacking angle. *Int J Agric & Biol Eng*, 2026; 19(1): 283–294.

1 Introduction

To meet the growing demands of modern agricultural machinery for high precision and efficiency, various design methods have been developed. Among them, simulation is a widely adopted method due to its reliable results and independence from weather conditions. Parameter calibration is a critical step in simulation studies and the core factor affecting simulation accuracy. DEM-based calibration has become a key aspect of the optimization process in agricultural machinery design. Through computer simulation technology, the working conditions of agricultural

machinery can be accurately modeled, allowing for in-depth analysis and optimization^[1-3]. In DEM parameter calibration, the critical tasks are determining the geometric model and simulation parameters. The geometric model involves generating the shape and filling it with particles. At the same time, simulation parameters comprise basic material properties, such as density, Poisson’s ratio, and shear modulus, as well as contact parameters, including static friction coefficient, rolling friction coefficient, and restitution coefficient. The accuracy of these parameters is vital for simulation precision and the effective optimization of agricultural machinery design^[4-6]. In agricultural production, crop-specific differences in shape models and parameters exist. Therefore, simulation of different crops requires individual parameter calibration, even across different varieties. Both domestic and international studies have performed DEM simulations for crops such as gice mixtures^[7], safflowers^[8], panax notoginseng root^[9], spinach^[10], and watermelon seeds^[11].

To improve the accuracy of DEM simulations, crop-specific parameter calibration has been widely conducted. Yu et al.^[12] performed a combination of bench and simulation experiments for notoginseng seeds in sowing experiments and identified optimal contact parameters between seeds and contact materials for DEM simulation. Li et al.^[13] conducted DEM parameter calibration for cottonseeds, using seed crushing force and energy as evaluation indices to determine the optimal combination of restitution, static

Received date: 2025-08-14 **Accepted date:** 2025-12-15

Biographies: **Changji Liu**, Postgraduate, research interest: precision seeding in arid areas, Email: 2678805978@qq.com; **Wuyun Zhao**, PhD, Professor, research interest: agricultural mechanization engineering, Email: zhaowuy@gsau.edu.cn; **Bin Feng**, PhD, Associate Professor, research interest: mechanized farming technology and theoretical direction, Email: 470236645@qq.com; **Bugong Sun**, PhD Professor, research interest: full mechanization of dryland farming, Email: sunbg@gsau.edu.cn; **Fei Dai**, PhD, Professor, research interest: mechanical engineering, Email: daifei@gsau.edu.cn; **Hui Li**, Postgraduate, research interest: precision seeding in arid areas. Email: lh2133996862@163.com.

***Corresponding author:** **Linrong Shi**, PhD, Associate Professor, research interest: research on key technologies and equipment for precision and intelligent seeding in Northwest China. College of Mechanical and Electrical Engineering, Gansu Agricultural University, Lanzhou 730070 China, Email: shilr@gsau.edu.cn.

friction, and dynamic friction coefficients that best represent the crushing-compression process of cottonseeds. Zhang et al.^[14] established a simulation model for mung bean seeds in sowing trials and obtained simulation parameters between mung beans and contact materials, providing theoretical guidance for the design and optimization of precision sowing devices. Xia et al.^[15] calibrated the flexible DEM model parameters for rice straw using the maximum bending load as the evaluation index, thereby determining the optimal contact parameters for straw return implements. Liu et al.^[16] calibrated parameters for coated corn seeds, using the error of the stacking angle as a response value, and optimized parameters using NSGA-II to obtain reliable and accurate contact parameters. Aorigele et al.^[17] used a combination of static stacking angle experiments and simulation experiments to calibrate simulation parameters, obtaining the optimal contact parameters between sunflower seeds and Q235 Steel, which were then applied to simulations of sunflower seed transportation to improve DEM accuracy.

In summary, the stacking angle serves as a comprehensive indicator that reflects the restitution coefficient, static friction coefficient, and rolling friction coefficient between particles, making it an effective metric for characterizing contact behavior among seed particles. Traditional approaches mainly rely on coupling physical and simulated static stacking angle experiments to determine key contact parameters and improve simulation precision. However, due to the flat wedge-shaped geometry of sunflower seeds, using a static stacking angle for calibration often leads to significant errors, thereby affecting the accuracy of parameter calibration. To enhance the accuracy of DEM-based sowing simulations for coated sunflower seeds and increase data diversity, this study adopts the dynamic stacking angle as the characteristic indicator. By integrating physical and simulation experiments, the key contact parameters are optimally calibrated. Additionally, factors such as the rotational speed of the container, the inner wall material of the drum, the seed volume ratio, and the seed variety are introduced as influencing variables, further improving the applicability and accuracy of contact parameter calibration^[18-21].

2 Materials and methods

2.1 Experimental materials

The experimental sunflower seeds used in this study included two varieties for comparative testing: “Xinhe No. 1” edible sunflower seeds, a locally common cultivar in the Gansu region, and “Chunyou No. 1” oil sunflower seeds. Both seed batches were sourced from a laboratory supplier. In addition, to carry out relevant mechanical property and stacking behavior tests of the sunflower seeds, three types of experimental containers with different inner wall materials were prepared for the experiment, namely containers with Q235 Carbon Steel inner walls, 304 Stainless Steel inner walls, and ABS Engineering Plastic inner walls. These containers were applied to subsequent tests including the dynamic stacking angle measurement.

For Xinhe No. 1, a random sample of 100 seeds was selected, and their three-dimensional parameters (length, width, and thickness) were measured using a digital Vernier caliper with a precision of 0.02 mm. The measurement results are presented in Figure 1, which demonstrates that the seed dimensional parameters conform to a normal distribution. As indicated in Figure 2 (where average length, width, and thickness are denoted as L , W , and T , respectively), Xinhe No. 1 had a mean length (L) of 20.19 mm

(variance=1.19), mean width (W) of 6.94 mm (variance=0.47), and mean thickness (T) of 3.34 mm (variance=0.48). The average bulk density of Xinhe No. 1 was determined via the water displacement method, yielding a value of 489 kg/m³. Its moisture content was verified as 9% per product specifications, and the average thousand-kernel weight was measured as 115.48 g using an electronic balance with 0.01 g precision. For Chunyou No. 1 oil sunflower, no dimensional calibration was conducted, so its three-dimensional parameters were not measured; the variety was only incorporated to support comparative experimental analysis of dynamic stacking angles between edible and oil sunflower seeds under the three aforementioned inner wall material conditions.

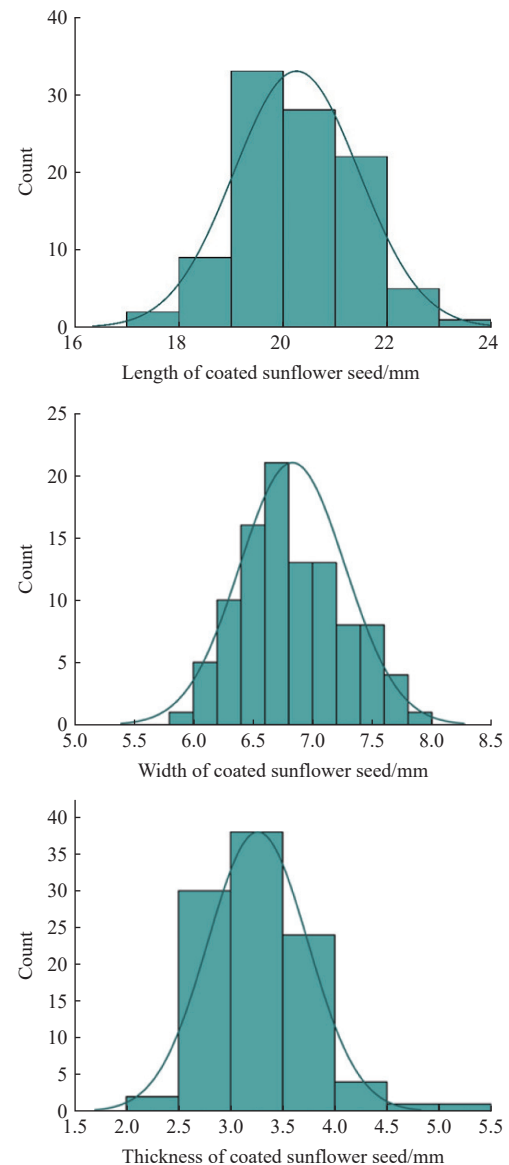


Figure 1 Normal distribution of seed length, width, and thickness

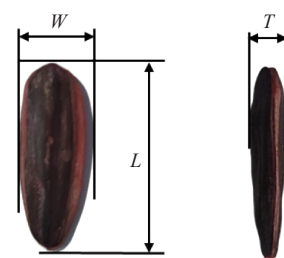


Figure 2 Shape and characteristic dimensions

2.2 Seed simulation model

Figure 3a presents the 3D model of the sunflower seed constructed in SolidWorks, which was established based on the measured three-dimensional parameters of the seeds. This 3D model was exported in STL file format and imported into EDEM software, where a discrete element model (DEM) was developed using the sphere-filling method. The number of filled spherical particles is a key factor affecting both simulation accuracy and computational efficiency: a smaller particle count enables faster computation but results in a model shape that deviates significantly from the actual seed geometry; conversely, increasing the particle number can more accurately approximate the seed's true shape, thereby improving simulation accuracy but reducing computational efficiency. Therefore, the particle-filling scheme was determined by balancing geometric fidelity and computational cost. As illustrated in Figure 3b, this configuration effectively reproduces the overall shape of the seed after spherical particle filling. As shown in Figure 3c, the seed model was filled with 32 spherical particles (radii ranging from 0.4 mm to 2.1 mm) that are uniformly distributed throughout the seed geometry.

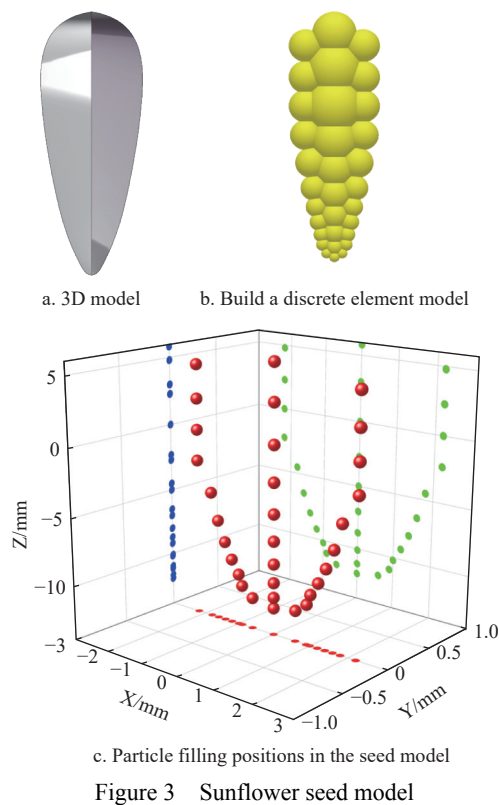


Figure 3 Sunflower seed model

2.3 Experimental methods

A rotary drum device was used to conduct the dynamic stacking angle experiment of seeds, aiming to determine the working conditions of the drum and to clarify the variation pattern of the dynamic stacking angle. The horizontal loading method was used to measure the static friction coefficient between the seeds and the contact material. The free-fall collision experiment was conducted to determine the restitution coefficient between seeds and between seeds and the contact material. A combination of simulation experiments and rotary drum experiments was employed to calibrate the rolling friction coefficient between seeds and the contact material, as well as the static and rolling friction coefficients between seeds and the contact material. A single-factor experiment was used to determine the reasonable range of calibration parameters. Taking the physical dynamic stacking angle as the

evaluation index, the contact parameters of seed particles in the discrete element model were optimized using the Design-Expert 13 software. The optimized parameter combination was validated through simulation using EDEM software. When the error between the simulated and experimental stacking angles fell within a reasonable range, the parameter calibration of the discrete element model for seeds was considered complete.

3 Dynamic stacking angle experiment of seeds

To investigate the effects of various factors on the dynamic stacking angle and to identify the associated variation patterns and optimal drum operation parameters, an experimental study was performed. The drum rotation speed, drum inner wall material, and seed volume filling ratio were selected as variable factors to analyze the effects of these external factors. Different seed varieties were introduced to conduct verification experiments. A rotary drum device with an inner diameter of 150 mm and an axial length of 200 mm was designed. The dynamic stacking angle of seeds inside the rotary drum is influenced by multiple factors, including intrinsic factors such as the inter-seed static friction coefficient and the inter-seed restitution coefficient, as well as extrinsic factors like contact material, drum rotation speed, drum inner wall material, and seed volume filling ratio.

The measurement device for the dynamic stacking angle of seeds is shown in Figure 4. Before the experiment, the inner wall material was replaced. During the experiment, the rotary drum device was adjusted to a horizontal position, with the center of the camera's field of view aligned with the center of the drum at a distance of 450 mm. The seeds were loaded into the rotary drum,

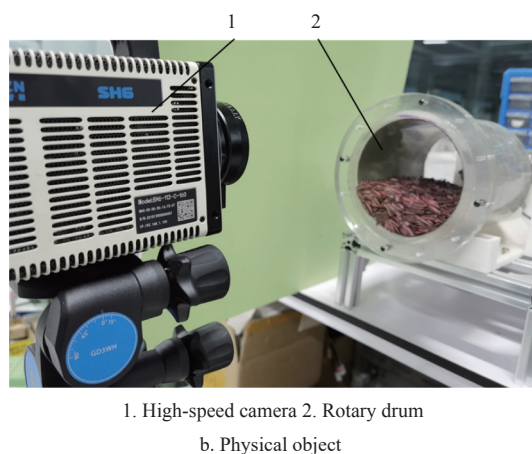
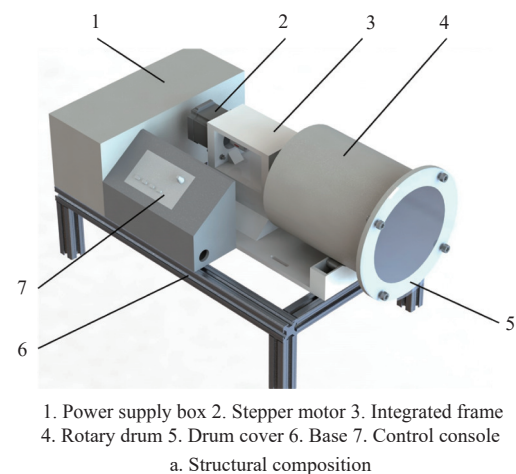


Figure 4 Measurement device for the dynamic stacking angle of seeds

the drum cover was secured, and the stepper motor was started. The drum rotation speed was controlled using the speed adjustment knob. Once the rotary drum operated stably, high-speed video was recorded using a DeepVision SH6-113 high-speed camera at 13 600 frames per second (fps) for 10 seconds. The PR and PS image processing software were used to determine the maximum inclination angle between the sloped surface of the seed pile before collapse and the horizontal plane. This value was taken as the dynamic stacking angle of the seed particles under the current conditions. Each experiment group was repeated five times, and the

average value was taken as the final result.

3.1 Effects of different factors on the dynamic stacking angle

3.1.1 Operating duration

The drum rotation speed was set to 10 r/min, with the inner wall of the drum made of 304 stainless steel, and the seed volume ratio was set to 30%. Two time stages were selected for analysis: the acceleration phase of the rotation speed and the steady-speed operation phase. A dynamic stacking angle experiment was conducted on the seeds. The experimental results are shown in [Figure 5](#).

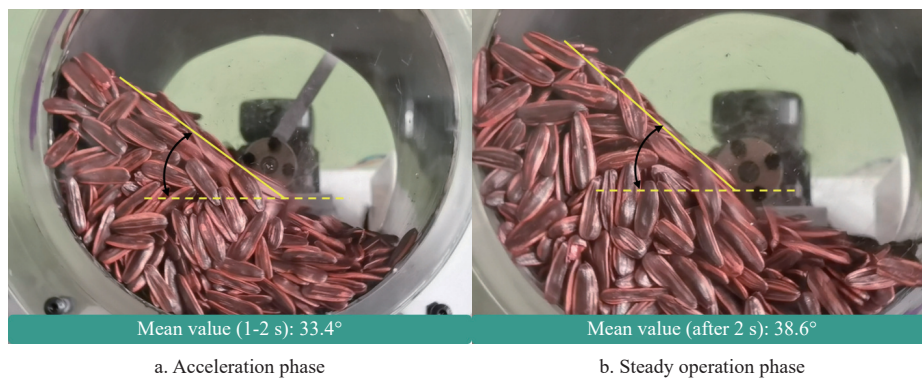


Figure 5 Time-varying dynamic stacking angle

As shown in [Figure 6](#), the dynamic stacking angle exhibits a non-monotonic evolution within 5 seconds. Starting from the initial state, the stacking angle increases rapidly to a peak within 0-2 s, reflecting the transient response of particles being rapidly excited and initially accumulated under external excitation. Subsequently, during the 2-5 s stage, the stacking angle gradually decreases and eventually stabilizes, indicating that the particle system reaches a dynamic flow equilibrium after structural rearrangement. This process clearly reveals the complete evolution of the material from a start-up transient state to steady flow.

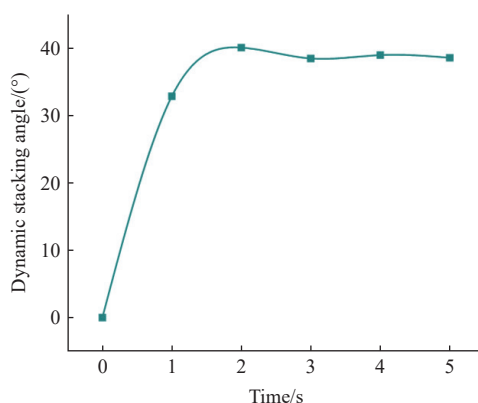


Figure 6 Dynamic stacking angle under varying operating times

3.1.2 Drum rotation speed, inner wall material, and filling ratio

The drum rotation speeds were set at 5 r/min, 10 r/min, and 15 r/min; the inner wall materials of the drum included Q235 Steel, 304 Stainless Steel, and ABS Plastic; and the seed filling ratios were set at 30%, 35%, and 40%. In all single-factor experiments, the fixed control parameters were kept consistent: the baseline drum rotation speed was set at 10 r/min, the inner wall material was fixed as 304 Stainless Steel, and the initial seed filling ratio was maintained at 30%. Single-factor experiments on the dynamic stacking angle were conducted separately for different rotation

speeds, different inner wall materials, and different filling ratios. The experimental results are shown in [Figure 7](#).

As shown in [Figure 8a](#), the rotation speed has a significant impact on the particle stacking state. As the rotation speed increases, the particles gain higher kinetic energy, which enhances the centrifugal force, leading to changes in particle distribution and stacking morphology, and thus increasing the dynamic stacking angle. At the same time, the friction and collisions between particles intensify at higher speeds, further increasing the stacking stability angle. Therefore, during the design and optimization of the seed calibration experiment's operating parameters, the influence of rotation speed on particle flow characteristics should be considered. A reasonable working speed should be set to prevent loss of control over particle flow and reduced stability due to excessively high speeds, thereby ensuring stable calibration data based on smooth flow.

As shown in [Figure 8b](#), the frictional properties of the inner wall material directly affect the stacking stability of particles within the drum. ABS, being a plastic material with a relatively smooth surface, allows particles to slide when in contact, leading to a lower stacking angle. The surfaces of Q235 Steel and 304 Stainless Steel are rougher, offering stronger frictional resistance, which inhibits particle sliding, promotes stacking stability, and increases the dynamic stacking angle. A comprehensive analysis suggests that in seed calibration experiment design, the appropriate lining material should be selected based on the physical properties of the particles and working conditions to ensure stable calibration data while maintaining a smooth flow.

As shown in [Figure 8c](#), when the filling ratio is low, insufficient seed filling leads to loose stacking, resulting in a smaller stacking angle. As the filling ratio increases, particle interaction intensifies, overall density increases, and changes in friction and support forces cause the angle to rise. At 40%, the particles tend to stack densely, with a significant increase in the angle, but the stability of the dynamic stacking angle decreases. In subsequent seed calibration experiments, an increase in the seed



Figure 7 Dynamic stacking angle under different factors

filling ratio enhances friction and support forces between particles, resulting in an increase in the stacking angle. Attention should be given to the stacking angle stability within the 30% to 35% filling ratio range. Combined with material flow properties, an appropriate experimental filling ratio should be selected to ensure stable calibration data while maintaining smooth flow.

3.1.3 Seed varieties

The rotation speeds of the drum were set at 5 r/min, 10 r/min, and 15 r/min, with the inner wall materials of the drum being Q235 Steel, 304 Stainless Steel, and ABS Plastic. The initial filling ratio of seeds within the drum was set at 30%. Two seed varieties, oil sunflower seeds and confectionary sunflower seeds, were selected for the experiments. Single-factor dynamic stacking angle experiments were conducted for various seed varieties to investigate the impact of external factors on the dynamic stacking angles of seeds with distinct physical characteristics. Oil sunflower seeds were used as the external factor in the comparative experiments without parameter calibration. (a, b, d) represent the group of differences between different varieties at different rotation speeds, while (b, c, e) represent the group of differences between different varieties under different inner wall materials. The experimental results are shown in Figure 9.

As shown in Figure 10a, with the change in rotation speed from 5 r/min to 15 r/min, the stacking angles of both confectionary sunflower seeds and oil sunflower seeds increased. The particles were subjected to increased external disturbances, resulting in a decrease in stacking stability, which required a larger stacking angle to maintain a stationary state. Within the same range of rotation speed changes, the increase in stacking angle for confectionary sunflower seeds was greater, and their flow behavior was more

responsive to changes in rotation speed compared to oil sunflower seeds. Confectionary sunflower seeds have larger, smoother surfaces, resulting in lower friction and interlocking forces between particles. Under the influence of centrifugal force and disturbances, particle sliding and structural breakdown occur, causing an increase in the stacking angle. In contrast, oil sunflower seeds have a more interlocking particle shape, providing a stable structure and stronger resistance to disturbances. Therefore, their stacking angle increases less and changes more slowly.

As shown in Figure 10b, for the three inner wall materials—Q235 Steel, 304 Stainless Steel, and ABS Plastic—the dynamic stacking angle of confectionary sunflower seeds decreased. A similar downward trend was observed for oil sunflower seeds. The results demonstrate that for seeds with significantly different physical properties, such as confectionary sunflower seeds and oil sunflower seeds, the dynamic stacking angle changes exhibit a high degree of consistency when external factors are changed. This indicates that under the experimental conditions and seed types studied, the influence of external factors on the dynamic stacking angle follows a stable pattern, which has not been significantly altered by the physical property differences between the two seed types. This stability in the external factors' effect on the dynamic stacking angle provides a stable foundation for subsequent calibration experiments.

3.2 Determination of drum rotation operation working parameters

Multi-external-factor coupling physical experiments were performed on a drum platform, with three materials commonly used in seed metering device components adopted as wall contact media to isolate material-specific impacts on dynamic stacking angle. The

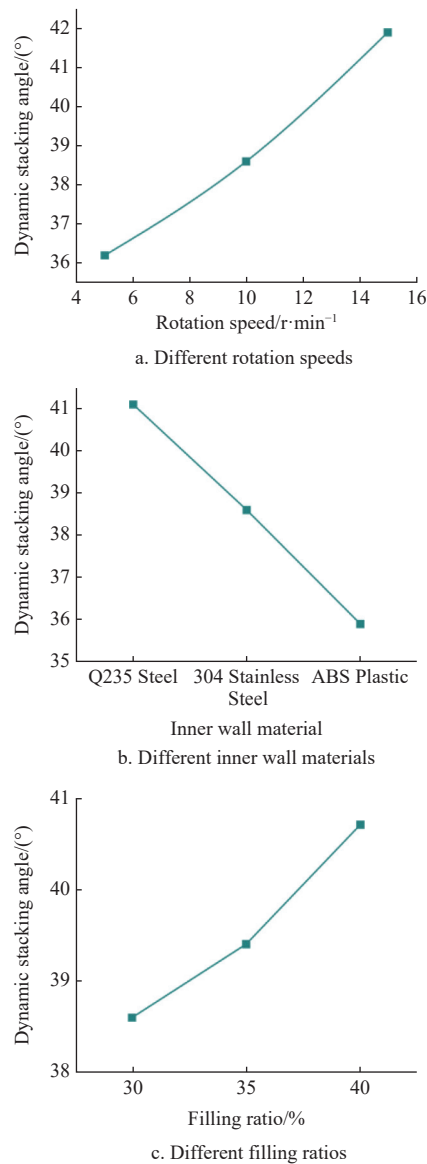


Figure 8 Effect of different parameters on the dynamic stacking angle

materials were selected for their relevance to seeding machinery applications: Q235 Steel (traditional seed metering cavity/conveying wall material, moderate surface roughness, high structural hardness), 304 Stainless Steel (precision corrosion-resistant component material, smooth, anti-oxidative surface), and ABS Engineering Plastic (lightweight hopper/chute material for specialty-crop seed meters, ultra-smooth surface). All specimens were fabricated to identical geometric dimensions, with surface properties pre-calibrated to eliminate dimensional or property variability, ensuring observed dynamic stacking angle variations originated from material characteristics rather than experimental artifacts. The experimental scheme was designed in Design-Expert software with dynamic stacking angle as the response variable; a multi-factor interaction model was established based on experimental data, and a multi-level scheme for parameters in Table 1 was developed via the Optimal Design module. Dynamic stacking angles of all groups (across the three contact materials) were measured and documented in Table 2. Analysis of variance (ANOVA) was conducted, where $p < 0.05$ indicated a statistically significant effect of external factors on dynamic stacking angle and $p < 0.001$ denoted a highly significant effect. By quantifying

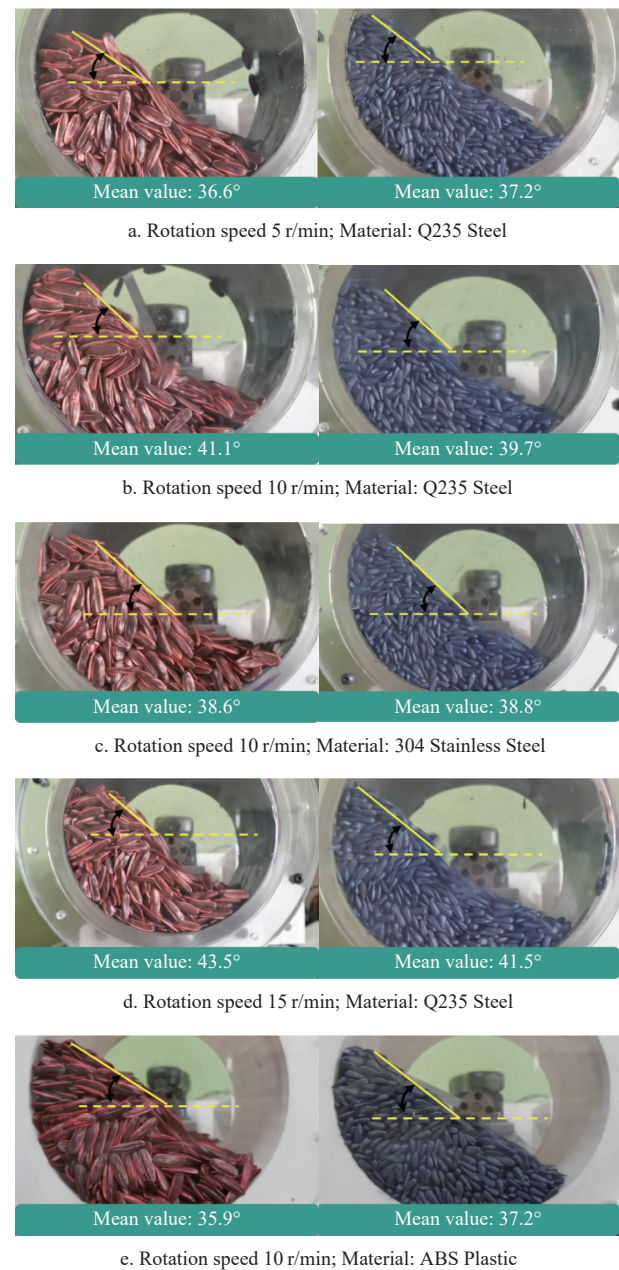


Figure 9 Dynamic stacking angles of different varieties

interactions among seed physical properties, external excitation, and contact material characteristics, the combined impacts on particle motion behavior were clarified, providing precise external factor conditions for contact parameter calibration.

This study integrated oil sunflower samples from comparative experiments into the multi-factor system to determine core parameters, exhibiting significant scientific rationality. As a typical sunflower seed material, oil sunflower kernel physical properties had been characterized in preliminary experiments. This design enabled same-system data collection, eliminating systematic errors from independent experiments, while oil sunflower data served as a benchmark for verifying parameter effectiveness. It also formed a closed-loop data system of “variety comparison–parameter optimization–mechanism verification”, which ensured experimental economy, guaranteed the final parameters’ variety adaptability and conclusion universality, and boosted the study’s scientific rigor and application value.

This study was based on the polyhedron solver function in EDEM and SolidWorks software was used to establish the three-

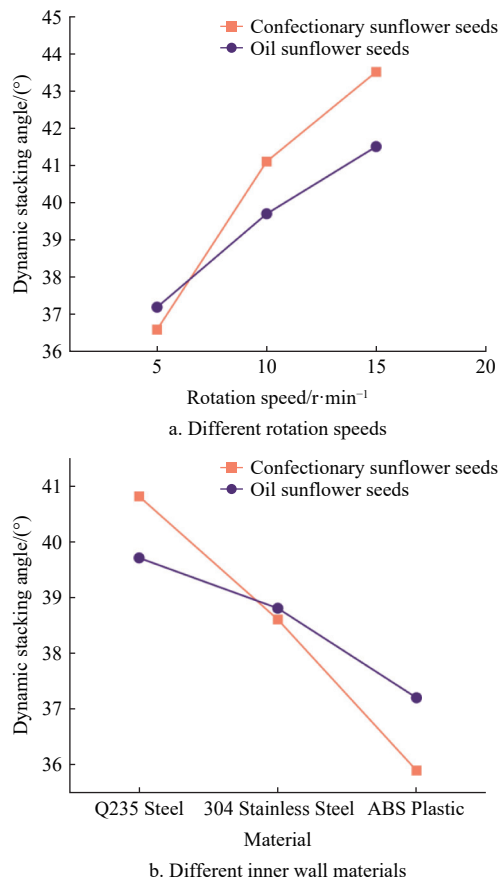


Figure 10 Effect of variety on dynamic stacking angle

Table 1 External factors and their levels

Factor	Level		
	-1	0	1
Seed variety, <i>A</i>	Confectionary Sunflower	-	Oil Sunflower
Drum rotation speed /r·min ⁻¹ , <i>B</i>	5	10	15
Inner wall material, <i>C</i>	ABS Plastic	Q235 Steel	304 Stainless Steel
Seed filling ratio, <i>D</i>	30%	-	35%

dimensional models of sunflower seeds and rollers, which were then imported into EDEM. Considering that there is almost no surface adhesion between sunflower seed particles and in line with the physical parameters of the sunflower seeds, the Hertz-Mindlin (no-slip) contact model was selected to reduce the computational load. Based on the data in Table 2, an analysis of variance (ANOVA) was conducted, and the results are listed in Table 3. Among the external factors, seed variety *A* ($p < 0.01$) had a significant effect on the dynamic stacking angle. Note: Oil sunflower seeds were used only as a comparison sample and were not included in the analysis. Both drum rotation speed *B* ($p < 0.001$) and inner wall material *C* ($p < 0.05$) had significant effects on the dynamic stacking angle of seeds, whereas seed filling ratio *D* ($p = 0.283$), within the range of 30% to 35%, did not show a significant effect.

Considering the significance level ($\alpha = 0.05$), effect size (F-value), and the experimental objective (dynamic stacking angle), the final selected conditions were: a rotation speed of 10 r/min, 304 Stainless Steel as the drum inner wall material, and a seed filling ratio of 30%. These parameter combinations were determined as the baseline experimental conditions for calibrating seed contact parameters.

Table 2 Experimental design and result parameters for dynamic stacking angle

No.	A	B/r·min ⁻¹	C	D/%	Dynamic stacking angle/(°)
1	Confectionary sunflower seeds	15	304	35%	39.74
2	Confectionary sunflower seeds	15	ABS	35%	38.88
3	Confectionary sunflower seeds	10	304	30%	38.20
4	Oil sunflower seeds	15	304	30%	41.08
5	Oil sunflower seeds	10	Q235	30%	39.74
6	Confectionary sunflower seeds	10	ABS	35%	35.92
7	Oil Sunflower seeds	10	304	35%	36.02
8	Oil Sunflower seeds	15	ABS	30%	38.52
9	Confectionary sunflower seeds	5	304	30%	32.04
10	Oil sunflower seeds	5	Q235	35%	36.12
11	Confectionary sunflower seeds	10	Q235	30%	36.20
12	Confectionary sunflower seeds	5	ABS	35%	37.02
13	Oil sunflower seeds	10	ABS	35%	29.70
14	Confectionary sunflower seeds	15	ABS	30%	40.64
15	Confectionary sunflower seeds	15	Q235	30%	46.52
16	Confectionary sunflower seeds	5	Q235	30%	42.58
17	Oil sunflower seeds	15	Q235	35%	44.14
18	Oil sunflower seeds	5	304	35%	35.04
19	Oil sunflower seeds	10	ABS	30%	38.56
20	Confectionary sunflower seeds	10	Q235	35%	39.34
21	Oil sunflower seeds	5	ABS	30%	35.26

Table 3 ANOVA of external factors

Experimental factor	Degrees of freedom	Sum of squares	F-value	<i>p</i> -value
A	1	6.45	8.32	0.011
B	2	142.83	15.67	<0.001
C	2	55.21	4.05	0.038
D	1	3.78	1.23	0.283

4 Calibration of seed contact parameters

During the operation of the seed metering device, the contact materials involved primarily include ABS Plastic, Q235 Steel, and 304 Stainless Steel. To conduct accurate discrete element simulations, this study determined the required key contact parameters as well as the parameters to be calibrated.

The calibration methods are as follows: the static friction coefficient between seeds and materials was directly measured using specialized instruments; the coefficient of restitution between seeds and materials was directly measured using the free-fall collision method. For the static friction coefficient between seeds, the rolling friction coefficient between seeds, and the rolling friction coefficient between seeds and materials, a simulation calibration method based on the dynamic stacking angle was employed. This method uses the dynamic stacking angle data obtained from rotary drum experiments as a benchmark. By adjusting the aforementioned parameters in the simulation, the simulated results were aligned with the physical experimental values, thereby inversely deriving the optimal parameter values. The discrete element simulation parameters for the interactions between seeds and contact materials are presented in Table 4^[21-23].

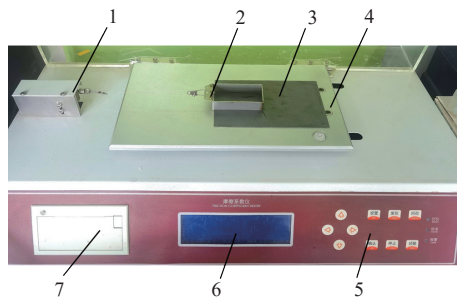
4.1 Static friction coefficient between seeds and contact materials

The static friction coefficient between seeds and contact materials was measured using the Saicheng MXD-02 static friction

coefficient experimenter, as shown in Figure 11. To ensure data accuracy and comparability, the instrument was checked for proper functioning before the experiment. The force sensor, tension module, and movable platform were inspected to confirm they were undamaged. The platform was kept clean, dry, and free from contaminants. A contact material with an area of 200 mm×200 mm was selected as the contact panel. During the experiment, the instrument was adjusted to remain level, and the contact panel was fixed onto the movable platform. The experimental values were selected through the display panel, and seeds with the same mass as the experiment object were added to the slider container. The experiment began, and the data were recorded and printed. Each set of experiments was repeated five times, and the average was taken to minimize measurement error. The results are listed in Table 5.

Table 4 Basic parameters for the discrete element method (DEM) simulation

Material	Parameter	Value
Seed	Poisson's ratio	0.35
	Density/kg·m ⁻³	489
	Shear Modulus/MPa	13
ABS Plastic	Poisson's ratio	0.39
	Density/kg·m ⁻³	1060
	Shear Modulus/MPa	890
Q235 Steel	Poisson's ratio	0.28
	Density/kg·m ⁻³	7850
	Shear Modulus/MPa	8.20×10 ⁴
304 Stainless Steel	Poisson's ratio	0.30
	Density/kg·m ⁻³	7800
	Shear Modulus/MPa	7.90×10 ⁴



1. Tension module 2. Slider container 3. Contact panel 4. Moving platform panel 5. Control panel 6. Display panel 7. Printing module

Figure 11 Static friction coefficient experiment

Table 5 Static friction coefficient between seeds and various contact materials

Material	Static friction coefficient	Coefficient of variation
Seed-304 Stainless Steel	0.32	10.23%
Seed-Q235 Steel	0.36	9.37%
Seed-ABS Plastic	0.25	9.16%

4.2 Coefficient of restitution between seeds and contact materials

The coefficient of restitution between seeds and contact materials was determined using the free-fall collision method^[24] with a drop height of 300 mm. As shown in Figure 12, before the experiment, a material panel with an area of 200×200 mm was fixed in place, and the seed release height was set as *H*. The maximum rebound height of the seed after contacting the material was denoted as *h*. A DeepVision SH6-113 high-speed camera was used for recording, with a frame rate of 13 600 frames per second (fps), to

capture the transient collision process synchronously. The highest rebound point of the seed was identified through video playback. The coefficient of restitution (*e*) is defined as the ratio of the relative velocity between the two objects after collision (*v*₀) to that before collision (*v*₁), as expressed in Equation (1). Each experiment was repeated five times, and the average value was calculated. The results are presented in Table 6.

$$e = \sqrt{\frac{v_0}{v_1}} = \sqrt{\frac{2gh}{2gH}} = \sqrt{\frac{h}{H}} \tag{1}$$

where, *e* is coefficient of restitution; *v*₀ is relative velocity after collision, m/s; *v*₁ is relative velocity before collision, m/s; *g* is gravitational acceleration, m/s²; *H* is seed release height, mm; *h* is maximum rebound height of seed and contact material, mm.

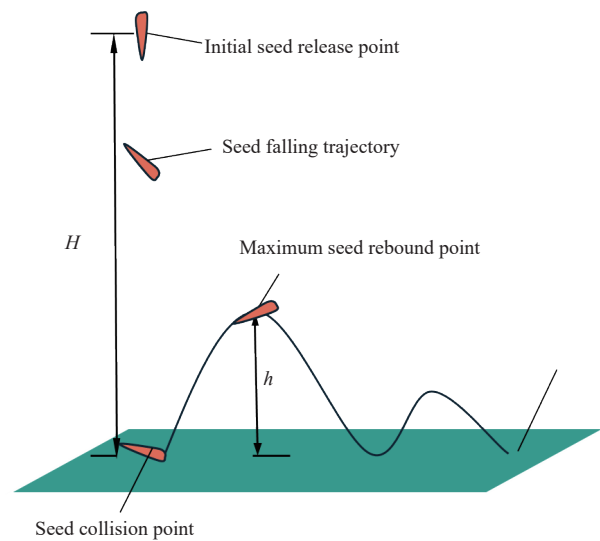


Figure 12 Schematic diagram of seed coefficient of restitution measurement

Table 6 Coefficient of restitution of each material

Material	Seed release height/mm	Coefficient of restitution	Coefficient of variation
Seed-304 Stainless Steel	300	0.42	12.39%
Seed-Q235 Steel	300	0.39	11.63%
Seed-ABS Plastic	300	0.32	13.16%
Seed-Seed	300	0.43	13.73%

4.3 Calibration of inter-seed contact parameters and inter-material rolling friction coefficient

When calibrating the contact parameters between sunflower seeds using traditional physical experiments, the seeds need to be attached to a base plate to form a seed plate. However, due to the flat and irregular shape of sunflower seeds, the resulting seed plate has significant inter-particle gaps and low surface flatness, leading to substantial experimental errors. The dynamic stacking angle is a characteristic parameter that comprehensively reflects the coefficient of restitution, static friction coefficient, and rolling friction coefficient between seed particles. A simulation model was constructed based on a rotating drum device and imported into EDEM software for discrete element simulation. During the simulation, the seed volume fraction and drum rotation speed were set according to the results of exogenous factor experiments to ensure realistic and accurate mechanical interactions. The contact behavior between sunflower seeds and 304 Stainless Steel was defined using the Hertz-Mindlin (no-slip) model to improve simulation accuracy. In the experiment, the coefficient of

restitution, static friction coefficient, and rolling friction coefficient between particles were selected as experimental factors. At the same time, the dynamic stacking angle was taken as the response indicator. A single-factor experiment was conducted to determine the range of values for each parameter. The multi-factor experimental data were then analyzed using an orthogonal experimental design, with regression analysis performed on the simulation results via Design-Expert 13 software. Subsequently, the parameter combination was optimized using a Box–Behnken design, and the optimal seed contact parameters were determined and validated through both simulation and physical experiments. Based on the obtained inter-seed contact parameters, the rolling friction coefficients between seeds and Q235 Steel and between seeds and ABS Plastic were further calibrated, followed by corresponding simulation and physical experiment validation.

4.3.1 Physical experiment on dynamic stacking angle

To accurately determine the dynamic stacking angle of sunflower seeds, seeds occupying 30% of the drum volume were placed inside a rotating drum. The drum was driven at a rotation speed of 10 r/min, and its inner wall was made of 304 Stainless Steel. Under the combined action of centrifugal force and gravity, the seed group reached a stable dynamic flow state. A DeepVision SH6-113 high-speed camera was used for recording, with a frame rate of 13 600 fps and a recording duration of 10 seconds. Image processing software PR and PS were used to analyze the video frames. The maximum inclination angle between the slope of the seed pile just before collapse and the horizontal plane was taken as the dynamic stacking angle of the seed particles under the given conditions. After five repeated measurements, the average dynamic stacking angle of the sunflower seeds was determined to be 38.6°.

4.3.2 Single-factor simulation experiment for parameter measurement

A single-factor simulation experiment was conducted to measure the influence of individual contact parameters on the dynamic stacking angle. The basic simulation parameters were set as follows: a drum rotation speed of 10 r/min, a drum material of 304 Stainless Steel, and a seed volume ratio of 30%. Detailed simulation parameters are listed in Table 7. Based on the morphological characteristics of sunflower seeds and literature review, the initial value ranges for parameter calibration were set as follows: Static friction coefficient between seeds: 0.2, 0.3, 0.4, 0.5, and 0.6. Rolling friction coefficient between seeds and 304 Stainless Steel: 0.01, 0.02, 0.03, 0.04, and 0.05. Rolling friction coefficient between seeds: 0.01, 0.02, 0.03, 0.04, and 0.05. Single-factor simulation experiments were conducted based on the above parameter settings. To ensure the independence of single-factor variable analysis, all non-variable contact parameters were held constant throughout the trials: the seed-seed static friction coefficient was fixed at 0.4, the seed-304 Stainless Steel rolling friction coefficient at 0.02, and the seed-seed rolling friction coefficient at 0.02.

With the aim of clarifying the independent effects of various contact parameters on the dynamic stacking angle of sunflower seeds, single-factor simulation experiments were conducted in this study. First, unified basic simulation conditions were set: a drum rotational speed of 10 r/min, a drum material of 304 Stainless Steel, and a seed volume fraction of 30%. Then, based on seed morphology and literature review, the initial value ranges of contact parameters were determined, while non-variable parameters were fixed at baseline values (seed-seed static friction coefficient of 0.4, seed-304 Stainless Steel rolling friction coefficient of 0.02, and seed-

seed rolling friction coefficient of 0.02). Subsequently, three groups of gradient repeated simulations and dynamic stacking angle data collection were carried out for seed-seed static friction (0.2-0.6), seed-Stainless Steel rolling friction (0.01-0.05), and seed-seed rolling friction (0.01-0.05), respectively.

Table 7 Single-factor simulation experiment parameters

Parameter	Unit	Value
Poisson's ratio of seed	-	0.35
Poisson's ratio of 304 Stainless Steel	-	0.30
Density of seed	kg·m ⁻³	489
Density of 304 Stainless Steel	kg·m ⁻³	7800
Shear modulus of seed	MPa	13
Shear modulus of 304 Stainless Steel	MPa	7.9×10 ⁴
Static friction coefficient between seed and 304 Stainless Steel	-	0.32
Coefficient of restitution between seed and 304 Stainless Steel	-	0.42
Coefficient of restitution between seeds	-	0.43

Based on the results of the single-factor simulation parameter experiments, the optimized inter-seed parameter ranges are: static friction coefficient between seeds: 0.30-0.50. Rolling friction coefficient between seeds: 0.01-0.03. Rolling friction coefficient between seeds and 304 Stainless Steel: 0.01-0.03.

4.3.3 Secondary orthogonal simulation experiment

Preliminary parameter measurement tests were conducted on the EDEM 2020 simulation platform. A polyhedral particle model of sunflower seeds was established in the software, and the Hertz-Mindlin (no bonding) contact model was adopted. With the simulation time step set to 1.5 μs and the total simulation duration to 10 s, the reasonable ranges of the inter-seed static friction coefficient, inter-seed rolling friction coefficient, and seed-304 Stainless Steel rolling friction coefficient were further determined. Based on these ranges, the factor levels of the simulation tests defined by the central composite design method are listed in Table 8. Taking the dynamic stacking angle as the response value, a three-factor three-level orthogonal test was designed using Design-Expert 13 software. Furthermore, with the dynamic stacking angle Y obtained from the simulation tests as the core evaluation index, a multivariate quadratic orthogonal combination test was carried out, which included a total of 17 sets of simulation tests (five sets of central point repeated tests were incorporated to verify data reliability). During the tests, the seed accumulation profile in the stable stage was extracted via the post-processing module of EDEM, and the stacking angle was calculated accordingly; the test results are presented in Table 9. Multiple regression analysis was performed on the test data to further determine the significance level of the influence of each contact friction factor on the dynamic stacking angle of sunflower seeds.

Table 8 Factors and levels of the simulation experiment

Factor	Level		
	-1	0	+1
Rolling friction coefficient between seed and 304 Stainless Steel, E	0.01	0.02	0.03
Static friction coefficient between seeds, F	0.30	0.40	0.50
Rolling friction coefficient between seeds, G	0.01	0.02	0.03

The experimental data were fitted using Design-Expert 13 software, and the regression equation of the seed particle stacking angle concerning the experimental factors was obtained as Equation (2):

$$Y = 46.69 + 0.64E + 3.74F - 0.74EG - 1.07FG - 1.52F^2 - 1.73G^2 \tag{2}$$

where, Y , E , F , and G represent the dynamic stacking angle, the rolling friction coefficient between seed and 304 Stainless Steel, the static friction coefficient between seeds, and the rolling friction coefficient between seeds, respectively. The analysis of variance (ANOVA) results for the regression equation of the seed particle stacking angle are listed in Table 10.

Table 9 Simulation experiment plan and results

No.	Parameter			Dynamic stacking angle/(°)
	E	F	G	
1	0.02	0.5	0.01	48.18
2	0.01	0.5	0.02	47.88
3	0.02	0.4	0.02	45.82
4	0.03	0.4	0.01	46.34
5	0.01	0.3	0.02	40.16
6	0.01	0.4	0.01	43.68
7	0.02	0.4	0.02	47.16
8	0.03	0.3	0.02	42.30
9	0.03	0.4	0.03	44.54
10	0.02	0.3	0.03	40.84
11	0.02	0.4	0.02	47.18
12	0.02	0.4	0.02	46.60
13	0.01	0.4	0.03	44.86
14	0.02	0.5	0.03	46.68
15	0.03	0.5	0.02	49.24
16	0.02	0.3	0.01	38.06
17	0.02	0.4	0.02	46.70

Table 10 Analysis of variance of regression equation

Source of variance	Sum of squares	Degrees of freedom	F	p
Model	145.99	9	51.53	<0.0001
E	3.3	1	10.49	0.0143
F	111.9	1	355.44	<0.0001
G	0.0545	1	0.173	0.6900
EF	0.0016	1	0.0051	0.9452
EG	2.22	1	7.05	0.0327
FG	4.58	1	14.55	0.0066
E^2	0.0451	1	0.1433	0.7163
F^2	9.71	1	30.84	0.0009
G^2	12.65	1	40.19	0.0004
Residua	2.2	7	-	-
Lack of fit	0.9777	3	1.06	0.4579
Pure error	1.23	4	-	-
Cor total	148.2	16	-	-

Note: $p < 0.01$ indicates a highly significant effect; $0.01 < p < 0.05$ indicates a significant effect.

The three-factor, three-level ANOVA results for the stacking angle indicate that the established regression model reached an extremely significant level ($p < 0.0001$), demonstrating clear statistical significance. This suggests that the model can effectively explain the variation of the dependent variable (stacking angle). The coefficient of determination (R^2) was 0.9851, the adjusted R^2 was 0.9660, and the predicted R^2 was 0.8815. The differences among these values were less than 0.2, indicating excellent goodness of fit and reliable predictive capability. The adequate precision value of 25.29 indicates an ideal signal-to-noise ratio, showing that the model is suitable for the optimization design within the

experimental space. Furthermore, the lack-of-fit test was not significant ($p = 0.4579 > 0.05$), indicating good agreement between the model and the experimental data, with no significant deviation.

Regarding the effects of the experimental factors: F had the most significant impact on the stacking angle ($p < 0.0001$) and was identified as the primary influencing factor; the rolling friction coefficient (E) also had a significant effect ($p = 0.0143 < 0.05$); the individual impact of factor G was not significant ($p = 0.6900 > 0.05$). For interaction effects, EG was substantial ($p = 0.0327 < 0.05$), and FG was highly significant ($p = 0.0066 < 0.01$), indicating synergistic effects between these factors. The nonlinear terms F^2 ($p = 0.0009$) and G^2 ($p = 0.0004$) were both less than 0.01, showing extreme significance, which suggests that the effects of these two factors exhibit nonlinear characteristics.

In summary, the model demonstrates excellent fitting performance and high prediction accuracy, providing a solid theoretical basis for subsequent optimization and parameter adjustment.

4.3.4 Optimization of optimal parameter combination

The rolling friction coefficient between particles had no significant effect on the dynamic stacking angle of seeds, and its value was relatively small in the actual simulation process; therefore, it was set to the minimum value of 0.010. To obtain the optimal combination of the rolling friction coefficient between seeds and 304 Stainless Steel and the static friction coefficient between seed particles that more closely matches the actual value, with a target dynamic stacking angle of 38.6°, the Optimization-Numerical module of Design-Expert 13 software was employed to perform multi-objective optimization on the fitted regression equation. The optimization objectives and constraint equations are as follows:

$$\begin{cases} Y(E, F, G) \\ E \in [0.01, 0.03] \\ F \in [0.3, 0.5] \\ G = 0.01 \end{cases} \tag{3}$$

By solving Equation (3), the optimal parameter combination was obtained: the rolling friction coefficient between seeds and 304 Stainless Steel, the static friction coefficient between seed particles, and the rolling friction coefficient between seed particles were 0.012, 0.31, and 0.010, respectively.

4.3.5 Experimental validation of physical and simulation results

Based on the optimized parameter combination, simulation experiments were conducted using EDEM software. Each experiment was repeated five times, and the average value was calculated. The resulting simulated stacking angle was 39.1°, with a relative error of less than 1.5% compared to the physical stacking angle. This indicates that the results of the simulation stacking experiments closely matched those of the physical experiments. The calibrated discrete element simulation contact parameters for seeds in this study can serve as a reference for the design and optimization of precision seeding machinery for coated sunflower seeds.

4.3.6 Rolling friction coefficient between seed particles and contact materials

Based on the previously determined rolling friction coefficient between seeds and 304 Stainless Steel, as well as the inter-seed contact parameters, this experiment focused on calibrating the rolling friction coefficients between seeds and Q235 Steel, as well as between seeds and ABS Plastic. As shown in Figure 13. In the experiment, the rolling friction coefficient was set as the

experimental factor, and the dynamic stacking angle was used as the response index. By combining discrete element simulation with physical experiments, the rolling friction coefficients between seeds and Q235 Steel and between seeds and ABS Plastic were ultimately determined.

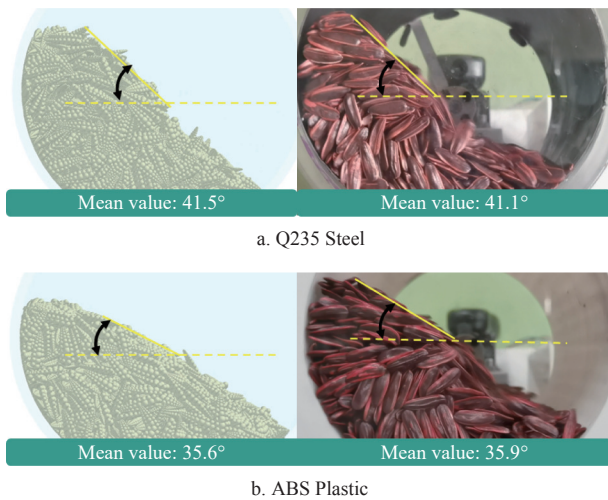


Figure 13 Comparison between simulated and measured stacking angles of seeds

Based on the analysis of data from both physical and simulation experiments, the rolling friction coefficients between seeds and Q235 Steel, as well as between seeds and ABS Plastic, were determined to be 0.011 and 0.010, respectively.

5 Conclusions

In this study, the coated sunflower seed variety “Xinhe No. 1” was selected as the experimental subject. A combination of physical and simulation experiments was employed to calibrate the contact parameters of the coated sunflower seeds. The main conclusions are as follows:

1) The three axial dimensions of “Xinhe No. 1” seeds followed a normal distribution. The average length was 20.19 mm with a variance of 1.19; the average width was 6.94 mm with a variance of 0.47; the average thickness was 3.34 mm with a variance of 0.48. The average thousand-kernel weight was 115.48 g, and the bulk density was 489 kg/m³.

2) The static friction coefficients between the coated sunflower seeds and 304 Stainless Steel, Q235 Steel, and ABS Plastic, measured using a static friction coefficient testing device, were 0.32, 0.36, and 0.25, respectively. Using a drop impact experiment, the restitution coefficients between the seeds and the four materials—304 Stainless Steel, Q235 Steel, ABS Plastic, and other seeds—were determined to be 0.42, 0.39, 0.32, and 0.43, respectively.

3) Taking the rolling friction coefficient between seed particles, the restitution coefficient, and the rolling friction coefficient between seeds and 304 Stainless Steel as experimental factors, and using the dynamic stacking angle as the response index, a three-factor, three-level response surface experiment was conducted using the cylinder rolling method. The contact parameters were optimized through modeling and verification using the EDEM simulation platform. The final calibrated parameters were: rolling friction coefficient between seeds and 304 Stainless Steel, 0.012; static friction coefficient between seeds, 0.31; and rolling friction coefficient between seeds, 0.010.

4) Taking the rolling friction coefficients between seeds and the

surfaces of Q235 Steel and ABS Plastic as experimental factors, and using the dynamic stacking angle as the response index, calibration experiments were conducted using the cylinder rolling method, followed by parameter optimization. By combining EDEM simulation experiments with physical experiments, the rolling friction coefficients between seeds and Q235 Steel and ABS Plastic were determined to be 0.011 and 0.010, respectively.

5) This study has the following limitations: the fixed inner wall structure of the experimental device is not conducive to material replacement and combination, which may affect result consistency; the accumulation angle relies on manual measurement, which is prone to subjective errors; the sample type is limited, and the simulation model is simplified, leading to a gap between experimental data and actual working conditions. To address these shortcomings, subsequent research can be improved in two aspects: first, by adopting a modular inner wall design to support material replacement and enhance the adaptability and reliability of the device; second, by introducing an intelligent vision system to achieve automatic tracking and extraction of accumulation parameters, thereby eliminating human errors and improving the objectivity, consistency, and experimental efficiency of the results.

Acknowledgements

This work was financially supported by the Fuxi Young Talent Cultivation Project of Gansu Agricultural University (Grant No. gaufx-05y02), the National Natural Science Foundation of China (Grant No. 52365030), the Science and Technology Innovation Fund of Gansu Agricultural University–Young Mentor Support Fund Project (Grant No. GAUQDFC-2024-06), the Construction Project of Gansu Dryland Agriculture Equipment Industry Research Institute, the Gansu Province Major Science and Technology Special Project (Grant No. 25ZDNF001-1), the Gansu Provincial Major Science and Technology Special Program (Grant No. 24ZD13NA019), the Gansu Provincial Industry-Academia-Research Integration and Technological Breakthrough Empowerment Program Project (Grant No. 25FNFF001-2), and the 2023 Gansu Provincial Agricultural Machinery R&D, Manufacturing, Promotion, and Application Integrated Pilot Project (3-3).

[References]

- [1] Li C F, Liu J F, Feng X J, Li J P. Modern machine design technique and agricultural machinery design. *Journal of Agricultural Mechanization Research*, 2006(5): 186–188. (in Chinese)
- [2] Wang L, He X W, Hu C, Guo W S, Wang X F, Xing J F, et al. Measurement of the physical parameters and calibration of discrete element simulation parameter of coated cotton seed. *Journal of China Agricultural University*, 2022; 27(6): 71–82. (in Chinese)
- [3] Chen L, Yu N H, Wang L Z, Fan J J, Lei G, Liu X P, et al. Measurement of contact parameters and discrete element simulation calibration of rice bran and broken rice. *Journal of Agricultural Science and Technology*, 2024; 26(2): 127–136. (in Chinese)
- [4] Shi L J, Yang M L. An analysis on research hotspots in agricultural engineering in China based on scientometrics. *Transactions of the Chinese Society of Agricultural Engineering*, 2016; 32(Z2): 430–438. (in Chinese)
- [5] Zeng Z W, Ma X, Cao X L, Li Z H, Wang X C. Critical review of applications of discrete element method in agricultural engineering. *Transactions of the Chinese Society for Agricultural Machinery*, 2021; 52(4): 1–20. (in Chinese)
- [6] Ma Z, Li Y M, Xu L Z. Summarize of particle movements research in agricultural engineering realm. *Transactions of the Chinese Society for Agricultural Machinery*, 2013; 44(2): 22–29. (in Chinese)
- [7] Yuan J B, Wang J F, Li H, Qi X D, Wang Y J, Li C. Optimization of the cylindrical sieves for separating threshed rice mixture using EDEM. *Int J Agric & Biol Eng*, 2022; 15(2): 236–247.

- [8] Zhang Z G, Zeng C, Xing Z Y, Xu P, Guo Q F, Shi R M, et al. Discrete element modeling and parameter calibration of safflower biomechanical properties. *Int J Agric & Biol Eng*, 2024; 17(2): 37–46.
- [9] Xie K T, Zhang Z G, Wang F A, Yu X L, Wang C L, Jiang S F. Calibration and experimental verification of discrete element parameters of *Panax notoginseng* root. *Int J Agric & Biol Eng*, 2024; 17(4): 13–23.
- [10] Zheng G, Qi B, Zhang W Y, Song S M, Wu Y, Xia Q Q, et al. Calibration and testing of discrete element simulation parameters for spinach seeds. *Computational Particle Mechanics*, 2025; 12: 479–490.
- [11] Wan Y, Zhang B W, Lai Q H, Gong Y, Qingxu Y, Chen X. Determination of melon seed physical parameters and calibration of discrete element simulation parameters. *Plos One*, 2024; 19: e0300516.
- [12] Yu Q X, Liu Y, Chen X B, Sun K, Lai Q H. Calibration and experiment of simulation parameters for *Panax notoginseng* seeds based on DEM. *Transactions of the Chinese Society for Agricultural Machinery*, 2020; 51(2): 123–132. (in Chinese)
- [13] Li Y C, Tian X L, Zhao Y, Liu X H, Zhou M L, Dai F S, et al. Parameter calibration and experiment of polyhedral cottonseed discrete element based on tavares model. *Transactions of the Chinese Society for Agricultural Machinery*, 2024; 55(7): 124–131, 220. (in Chinese)
- [14] Xia J F, Zhang P, Yuan H W, Du J, Zheng K, Li Y F. Calibration and verification of flexible rice straw model by discrete element method. *Transactions of the Chinese Society for Agricultural Machinery*, 2024; 55(9): 174–184. (in Chinese)
- [15] Liu R, Li Y J, Liu Z J, Liu L J, Lyu H T. Analysis and calibration of discrete element parameters of coated maize seed. *Transactions of the Chinese Society for Agricultural Machinery*, 2021; 52(S1): 1–8, 18. (in Chinese)
- [16] Ao R G L, Zhang W J, Wang S, Liu W H, Yu Z H. Measurement of physical contact parameters and discrete element simulation calibration of sunflower seeds. *Journal of Agricultural Mechanization Research*, 2023; 45(4): 139–147. (in Chinese)
- [17] Feng J X, Lin J, Li S Z, Zhou J Z, Zhou Z X. Calibration of discrete element parameters of particle in rotary solid state fermenters. *Transactions of the Chinese Society for Agricultural Machinery*, 2015; 46(3): 208–213. (in Chinese)
- [18] Santos K G, Campos A V P, Oliveira O S, Ferreira L V, Francisquetti M C, Barrozo M A S. DEM simulations of dynamic angle of repose of acerola residue: A parametric study using a response surface technique. *Blucher Chemical Engineering Proceedings*, 2015; 1(2): 1–8.
- [19] Cai W Y, Wang L Q, Xu L M. Discrete elemental parameter calibration of ultrafine calcium carbonate based on static and dynamic angle of repose. *China Powder Science and Technology*, 2024; 30(4): 81–93. (in Chinese)
- [20] Wu Z, Wang L Q, Xu L M, Gao W J. Discrete element parameters calibration of titanium dioxide based on static and dynamic repose angles. *China Powder Science and Technology*, 2023(4): 108–119. (in Chinese)
- [21] Yan J W, Wei S, Zhang W P, Zhang F G. Calibration of discrete element contact parameters for white radish seed particles. *Journal of Chinese Agricultural Mechanization*, 2023; 44(8): 1–11. (in Chinese)
- [22] Shi L R, Ma Z T, Zhao W Y, Yang X P, Sun B G, Zhang J P. Calibration of simulation parameters of flax seeds using discrete element method and verification of the seed-metering experiment. *Transactions of the Chinese Society of Agricultural Engineering*, 2019; 35(20): 25–33. (in Chinese)
- [23] Zhang W J, Yang M, Zhang Q L, Wang Q Z, Li X J, Bi Y, et al. Discrete element simulation parameter calibration and experimental verification of sea buckthorn material. *Journal of Northeast Agricultural University*, 2023; 54(10): 59–69. (in Chinese)
- [24] Ma Y C, Wang Z, Shi L R, Zhao W Y, Sun B G, Dai F, et al. Determination the intrinsic parameters and calibration of contact parameters for wheat seed particles. *Journal of China Agricultural University*, 2025; 30(3): 175–184. (in Chinese)